Journal : Small 11069 | Dispatch : 20-10-2015 | Pages : 27
Article No. : 2054 | LE | TYPESET
MS Code : NHAZ-D-14-00165 | CP | DISK

Nat Hazards
DOI 10.1007/s11069-015-2054-6

ORIGINAL PAPER

Enhanced paleoseismic succession at the Concud Fault (Iberian Chain, Spain): new insights for seismic hazard assessment

José L. Simón[1] · Luis E. Arlegui[1] · Lope Ezquerro[1] · Paloma Lafuente[1] · Carlos L. Liesa[1] · Aránzazu Luzón[1]

Received: 14 February 2014 / Accepted: 14 October 2015

Abstract A new trench excavated at the southern sector of the Concud Fault provided evidence of three paleoseismic events dated to ca. 21, 18 and 13–3 ka BP, respectively. The two youngest ones had not been detected in previous studies. The results extend the total recorded paleoseismic succession for the fault: eleven events since ca. 74 ka BP to the present day, with an average recurrence period between 7.1 ± 3.5 and 8.0 ± 3.3 ka; total net accumulated slip of about 20.5 m, with average coseismic slip of 1.9 m. The displacement pattern shows alternating periods of fast slip (up to 0.53 mm/a) and slow slip (0.13 mm/a), resulting in average slip rate of 0.29 mm/a. Using this paleoseismic information, as well as the potential magnitude previously attributed to the characteristic earthquake at the Concud Fault ($M \approx 6.5$–6.6), a simple probabilistic seismic hazard analysis has been performed. The estimated probability of occurrence of the characteristic earthquake within the next 500-year period ranges from 2.3 to 26.1 %, according to distinct hypotheses on the elapsed time derived from the uncertainty about the age of the youngest event.

✉ Paloma Lafuente
palomalaf@gmail.com

José L. Simón
jsimon@unizar.es

Luis E. Arlegui
arlegui@unizar.es

Lope Ezquerro
lope@unizar.es

Carlos L. Liesa
carluis@unizar.es

Aránzazu Luzón
aluzon@unizar.es

[1] Department Ciencias de la Tierra, Universidad de Zaragoza, C/Pedro Cerbuna 12, 50009 Saragossa, Spain

Journal : Small 11069 | Dispatch : 20-10-2015 | Pages : 27
Article No. : 2054 | LE | TYPESET
MS Code : NHAZ-D-14-00165 | CP | DISK

Keywords Concud Fault · Iberian Chain · Active tectonics · Paleoseismology · Seismic hazard · Intraplate seismicity

1 Introduction

AQ3 A common approach for assessing seismic hazard passes through the accurate modelling of past seismic patterns, driven by the assumption that large, characteristic seismic events represent ruptures of the same fault segment with the same coseismic slip and hence the same magnitude (Schwartz and Coppersmith 1984). Given long-term strain rate and constant stress distribution, it follows that characteristic earthquakes would occur at approximately equal intervals. This pattern permits to apply conditional probability procedures that, in turn, provide the likelihood that such an event will occur within a discrete time window (Schwartz and Coppersmith 1984; Yeats et al. 1997).

One of the requirements to perform this procedure is to know the date of the latest seismic event (*elapsed time*). In areas of intense seismicity, low recurrence intervals guarantee that the instrumental, at the worst the historical, record will provide the needed date. On the contrary, regions of low seismicity show larger recurrence intervals and this may imply very well that the latest event could be older than the existing records. This is the case of most intraplate areas, where active faults have large recurrence periods (in the order of 10^3 years; Liu and Zoback 1997) that are seldom considered in seismic hazard assessment. In such regions, studying the geological record for detecting and dating large ancient quakes by means of paleoseismological methods is therefore a critical task (Allen 1986; McCalpin 1996; Yeats et al. 1997).

The Iberian Chain, an intraplate range in eastern Spain, contains a number of active, geologically well-documented faults. The most important ones belong to the intramountain Jiloca Graben (Calamocha, Sierra Palomera and Concud faults) and Teruel Graben (El Pobo, Teruel and Valdecebro faults; Figs. 1, 2).

Nevertheless, historical and instrumental seismicity of this region is low to moderate (Fig. 2). Epicentres are concentrated (1) close to its western margin; (2) in the relay zone between Concud and Sierra Palomera faults; (3) in the Albarracín massif, W of the graben, and (4) in the area south of Teruel. No significant epicentre clustering occurs along the Concud Fault. Measured magnitudes (Mb) usually range from 1.5 to 3.5, with maximum Mb = 4.4 in the Teruel Graben and Mb = 3.8 in the Albarracín massif (data from IGN 2010). Before the instrumental period, intensities up to VI–VII were recorded in the Albarracín massif (1848), IV–V in the Jiloca Graben (1828) and VIII in the southern Teruel Graben (1656) (Mezcua and Martínez-Solares 1983). Focal depths are always less than 25 km and typically range from 5 to 15 km. This depth corresponds to the brittle layer above the basal detachment level, which is 10–15 km deep, according to Roca and Guimerà (1992). Most of the available focal mechanisms correspond to normal faults and are consistent with the recent regional stress field (Herraiz et al. 2000).

The best documented active fault during Pleistocene times is the Concud Fault. This structure has been an object of preliminary paleoseismological characterisation (Simón et al. 2005), morphotectonic analysis (Lafuente et al. 2012), as well as trenching studies (four trenches surveyed at its central and southern sectors, see Figs. 3 and 5; Gutiérrez et al. 2008; Lafuente et al. 2011a, 2014). The results allowed classifying the Concud Fault as a moderately active fault, with recurrent slip since early Late Pleistocene times and maximum

Journal : Small 11069 | Dispatch : 20-10-2015 | Pages : 27
Article No. : 2054 | LE | TYPESET
MS Code : NHAZ-D-14-00165 | CP | DISK

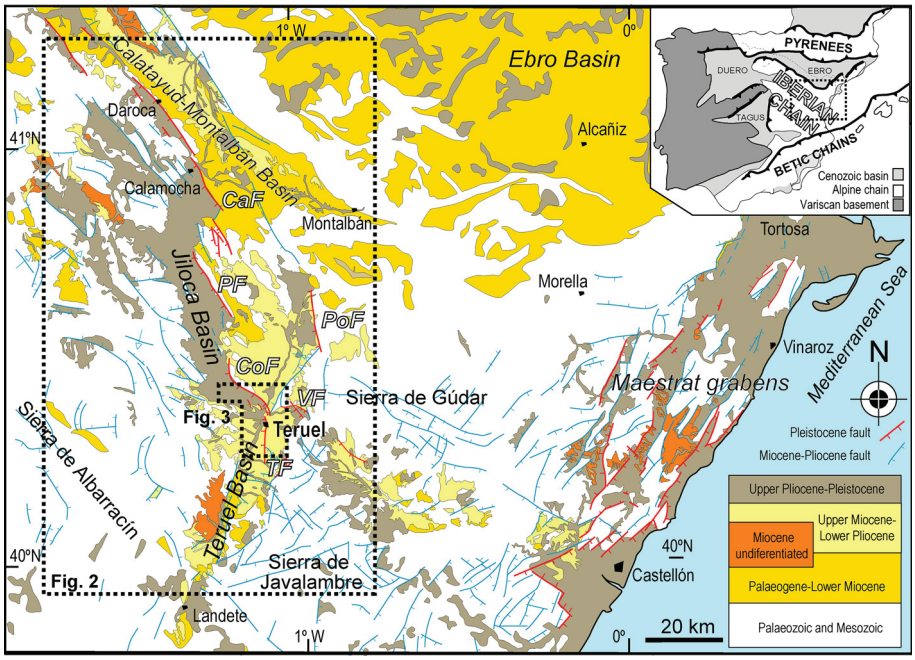

Fig. 1 Neogene-Quaternary extensional basins and main active faults in the central–eastern Iberian Chain. *CaF* Calamocha Fault, *PF* Sierra Palomera Fault, *CoF* Concud Fault, *PoF* Pobo Fault, *FT* Teruel Fault, *VF* Valdecebro Fault. *Inset* location of the study area within the Iberian Peninsula. Location of Figs. 2 and 3 is shown

estimated moment magnitude (Mw) in the range of 6.4–6.8 (Lafuente 2011; Lafuente et al. 2011a), although no historical destructive earthquake is linked to it. On the other hand, there is a gap of information corresponding to the latest Pleistocene and Holocene, and the hypothesis of additional events not recorded in the previously surveyed trenches has been seriously considered (Lafuente 2011; Lafuente et al. 2014). Searching for new evidence of younger paleoseismic events not yet documented is therefore a critical target.

This paper shows the results of a new trench excavated at the southern sector of the Concud Fault. After comparison with previous results, we are able to refine the paleoseismic succession for Late Pleistocene times and to improve our knowledge of the fault activity pattern. This is then applied to better assess the seismic hazard in Teruel, a city with about 35,000 inhabitants located only 3 km south of the surveyed site.

Also the Teruel Fault, in the neighbourhood of the Concud Fault (Fig. 3), has been object of paleoseismological research. Although evidence of four events occurred between 70.7 ± 5.3 and 9.9 ± 0.7 ka BP has been found (Simón et al. in preparation), timing of individual events is not well constrained; the overall Quaternary activity is poorly documented indeed, owing to the extreme scarcity of Quaternary deposits affected by this fault. Therefore, this fault has not provided enough data for being incorporated to seismic hazard analysis made in this paper, so that our present results are based on the Concud Fault as the only seismic source. Trench study in progress in the Teruel Fault and other active fault zones (Sierra Palomera and Valdecebro, see Figs. 1, 2) will allow to know more about paleoseismicity of the region and to achieve more refined seismic hazard assessment in the near future.

Journal : Small 11069 | Dispatch : 20-10-2015 | Pages : 27
Article No. : 2054 | LE | TYPESET
MS Code : NHAZ-D-14-00165 | CP | DISK

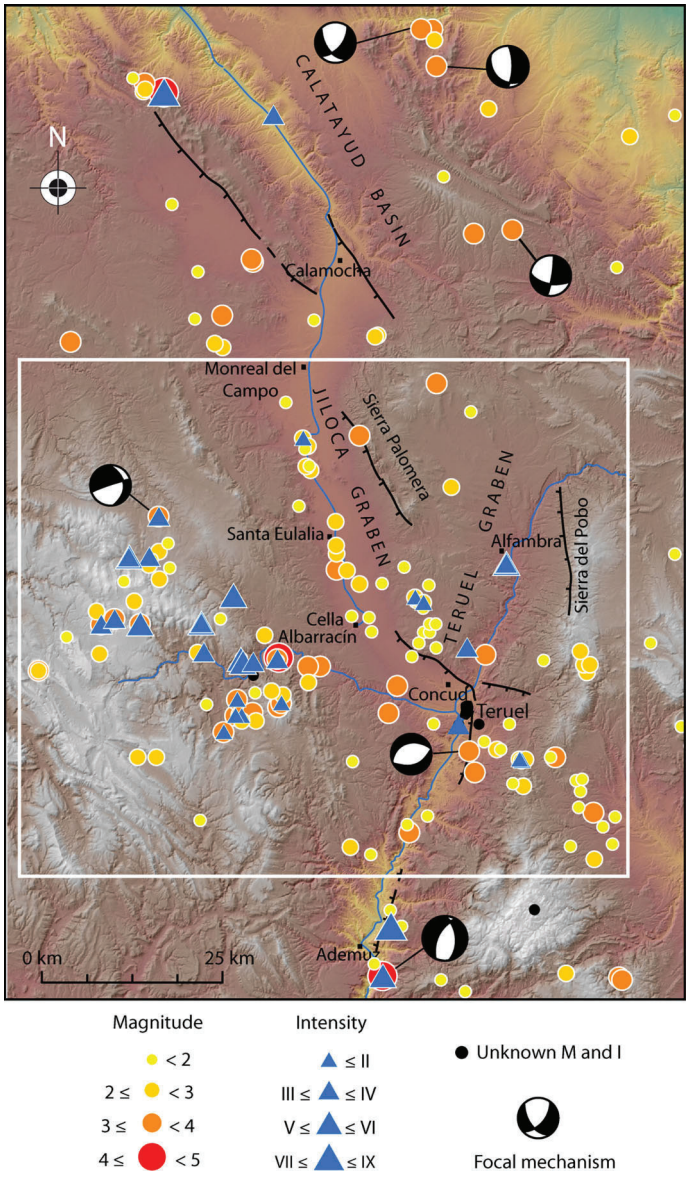

Fig. 2 Digital elevation model displaying epicentres of historical and instrumental earthquakes recorded in the Jiloca and Teruel grabens (DEM from SITAR, Aragón Regional Government). Seismic data from IGN (2010). The *squared area* includes historic and instrumental seisms computed in Fig. 12

2 Geological and structural setting

The central–eastern Iberian Chain includes a number of Neogene-Quaternary extensional basins that represent the onshore deformation of the Valencia Trough (Simón 1989; Roca and Guimerà 1992) and postdate the Alpine compressive structures (Fig. 1). The most

Journal : Small 11069 | Dispatch : 20-10-2015 | Pages : 27
Article No. : 2054 | LE | TYPESET
MS Code : NHAZ-D-14-00165 | CP | DISK

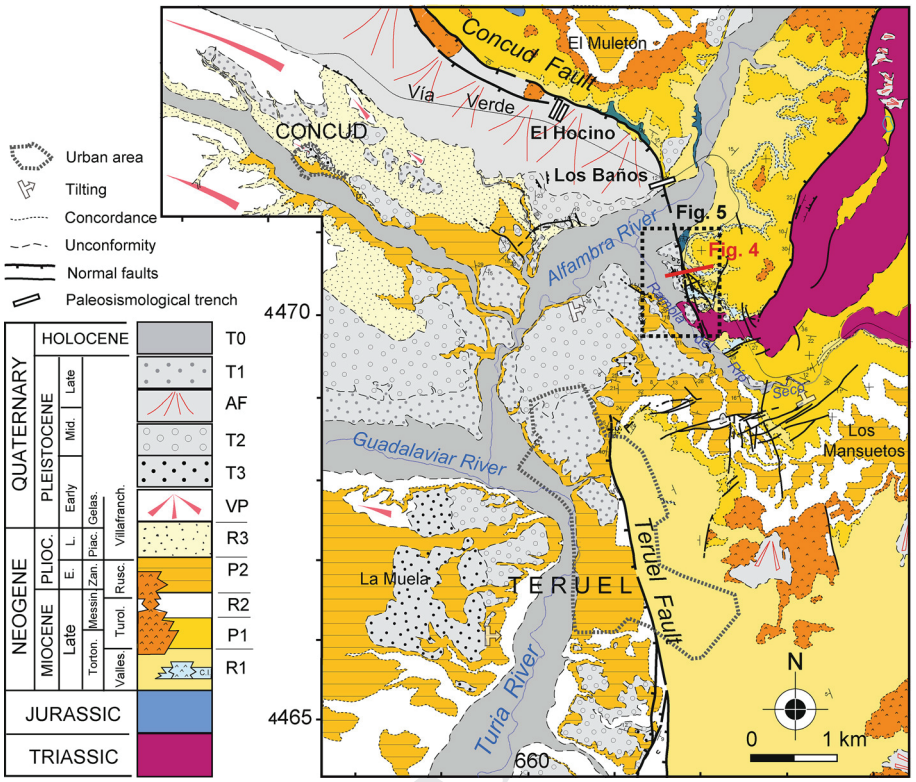

Fig. 3 Geological map of the Concud Fault showing the location of the studied area. R1: Vallesian clastics (Rojo 1), with interbedded limestone and gypsum; P1: Turolian carbonates (Páramo 1); R2: Turolian clastics (Rojo 2); G2: Tortajada and Los Aljezares gypsum units; P2: Ruscinian carbonates (Páramo 2); R3: Villafranchian clastics and carbonates (Rojo 3); VP: Villafranchian pediment; T3: Early Pleistocene terrace; T2: Middle Pleistocene terraces; F: Middle–Late Pleistocene alluvial fans; T1: Late Pleistocene terraces and local pediments; T0: Holocene terrace

recent extensional episode (Late Pliocene–Quaternary) gave rise to the NNW-SSE trending Jiloca Graben and reactivated other grabens (Teruel and Maestrazgo basins) generated in the previous episodes. These structures developed under a regional stress field that has been characterised as a nearly 'multidirectional' tension (σ_1 vertical, $\sigma_2 \approx \sigma_3$) with trajectories of the minimum stress σ_3 mainly trending ENE–WSW (Simón 1989; Arlegui et al. 2005).

The Teruel Basin is a half graben with an active eastern boundary made of large, nearly N–S striking faults (Fig. 1), filled with Neogene red clastic alluvial deposits that grade laterally into lacustrine evaporites and carbonates. The age of this infill is well constrained from numerous mammal fossil localities (Godoy et al. 1983a, b; Alcalá et al. 2000), ranging from the early Late Miocene (Vallesian) to the Late Pliocene–earliest Pleistocene (Villafranchian).

The asymmetric Jiloca Graben shows an overall NNW-SSE trend that results from en-echelon, right releasing arrangement of NW–SE striking normal faults, the largest ones being located at the eastern boundary: Calamocha, Sierra Palomera and Concud faults

Journal : Small 11069 | Dispatch : 20-10-2015 | Pages : 27
Article No. : 2054 | LE | TYPESET
MS Code : NHAZ-D-14-00165 | CP | DISK

(CaF, PF and CoF in Fig. 1). It is filled with Upper Pliocene to Pleistocene deposits corresponding to alluvial fans, pediments and episodic palustrine environments. In the central sector, these deposits are underlain by lacustrine/palustrine marls of a probable Neogene age (only observed in boreholes; Rubio and Simón 2007).

The Concud Fault is the southernmost fault bounding the Jiloca Graben and represents the negative inversion of a previous reverse fault (Lafuente 2011; Lafuente et al. 2011a). The trace is 14.2 km long and shows an overall NW–SE strike that veers towards N–S near its southern tip (Fig. 3); such change in orientation does not involve any structural or seismic segmentation (Lafuente et al. 2011a, b). The fault surface, typically dipping about 70°SW, puts into contact Pleistocene alluvial deposits in the hanging wall with either Triassic and Jurassic units (western and central sectors) or Neogene units belonging to the Teruel Basin (southeastern sector). At its SE tip, it approaches the neighbouring Teruel Fault, both showing a right relay arrangement and behaving as independent structures from a geometrical and kinematical point of view (Lafuente et al. 2011b). The kinematic analysis indicates a nearly pure normal movement on the main, NW–SE striking fault segment, while the slip vector on the southern, NNW–SSE striking segment shows a small left-lateral component (striation pitch around 75°S). These kinematical data result in a constant transport direction of the hanging wall towards N 220°E, which indicate that both segments show a complete kinematical compatibility (Lafuente et al. 2011b).

The extensional activity of the Concud Fault, as far as it has been geologically documented, began by the latest Ruscinian (mid-Pliocene), cutting the Upper Miocene–Lower Pliocene infill of the Teruel Basin (Fig. 3). Since that time, sedimentation was interrupted on the footwall, whereas a complete syntectonic sequence belonging to the Upper Pliocene and Quaternary was deposited on the hanging wall (Moissenet 1982; Simón 1983). The Upper Pliocene series includes red, fine-grained alluvial sediments with interbedded lacustrine–palustrine carbonates and is capped by a pediment cover (*Villafranchian pediment*). The Quaternary deposits are associated with: (1) fluvial terraces of the Guadalaviar and Alfambra rivers, some of them present as well in the footwall: upper terrace (T3), middle terrace (T2; Middle Pleistocene), lower terraces (three sublevels, T1a, T1b and T1c; Late Pleistocene) and Holocene terrace/flood plain (T0); (2) short alluvial fans developed from the fault scarp and spreading towards SW, mostly Late Pleistocene in age (Gutiérrez and Peña 1976; Peña 1981; Godoy et al. 1983a, b; Peña et al. 1984; Lafuente 2011).

The average slip rate for the overall extensional history of the Concud Fault can be calculated from the position and age of the youngest pretectonic level, i.e. the top of the Early Pliocene lacustrine deposits at the footwall (Godoy et al. 1983a, b). This level contains fauna belonging to the mammal zone MN 15b (latest Ruscinian; ca. 3.6 Ma; Godoy et al. 1983a, b; Opdyke et al. 1997; Alcalá et al. 2000) and shows a minimum vertical offset of about 240 m (Fig. 4). Considering an average dip of 70° and a pure normal movement, this results in a net displacement of 255 m, which could increase up to 290–300 m if we take into account the probable rollover geometry at depth. The resulting slip rate is 0.07–0.08 mm/a (Simón et al. 2005; Lafuente 2011; Lafuente et al. 2011a).

3 Methodology

Detailed geological and geomorphological mapping of the southernmost sector of the Concud Fault was carried out to find the suitable place for trenching. This was complemented with topographical and geophysical surveys. Deploying magnetic, electromagnetic

Journal : Small 11069 | Dispatch : 20-10-2015 | Pages : 27
Article No. : 2054 | LE | TYPESET
MS Code : NHAZ-D-14-00165 | CP | DISK

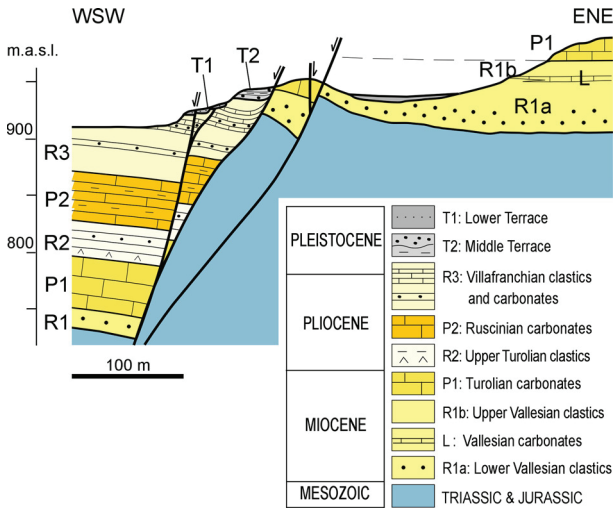

Fig. 4 Geological cross section at the southern sector of the Concud Fault (see location in Fig. 5a)

and ground-penetrating radar (GPR) methods were use to detect the fault under the soil or superficial regolith.

Classical trench methodology was applied to the selected site: excavating and shoring, cleansing and gridding the most suitable wall, identifying and marking sedimentary boundaries and faults, taking photographs, recording structural and sedimentological information and sampling relevant materials for OSL dating. Sedimentary units were defined on the basis of lithology, bed geometry, texture, colour and sedimentary structures. In addition, grain size distribution and mineralogical composition of two conspicuous silty levels were determined in order to constrain the correlation of units across the fault (Ezquerro et al. 2014).

After comparing the results in the new trench with those obtained from the previous works, a paleoseismic succession has been reconstructed for the Concud Fault. This provides (within an uncertainty range) the parameters needed for calculating probabilistic seismic hazard based on the concept of characteristic earthquake (Schwartz and Coppersmith 1984). The frequency distribution of recurrence intervals between characteristic earthquakes is the basis of such probabilistic hazard analysis. Several models of statistical distribution have been applied to this problem, the differences arising, quite often, from the source of data (instrumental vs. paleoseismic) and the assumed fault recurrence behaviour (Rhoades and van Dissen 2003; McCalpin 2009). Amongst them, the Gaussian distribution is preferred when the recurrence interval is nearly constant, but exhibits some variability (renewal or real-time models, Schwartz and Coppersmith 1986), and the data set is not large enough to solidly point to a different distribution (McCalpin 2009); therefore, this is quite often the distribution of choice in paleoseismology. Assuming a probabilistic Gaussian distribution of interseismic periods, the probability of occurrence of a seism equivalent to the characteristic earthquake in a given term (500 years) has been calculated according to the procedure proposed by Schwartz and Coppersmith (1986). The conditional probability (P) is defined as:

Journal : Small 11069 | Dispatch : 20-10-2015 | Pages : 27
Article No. : 2054 | LE | TYPESET
MS Code : NHAZ-D-14-00165 | CP | DISK

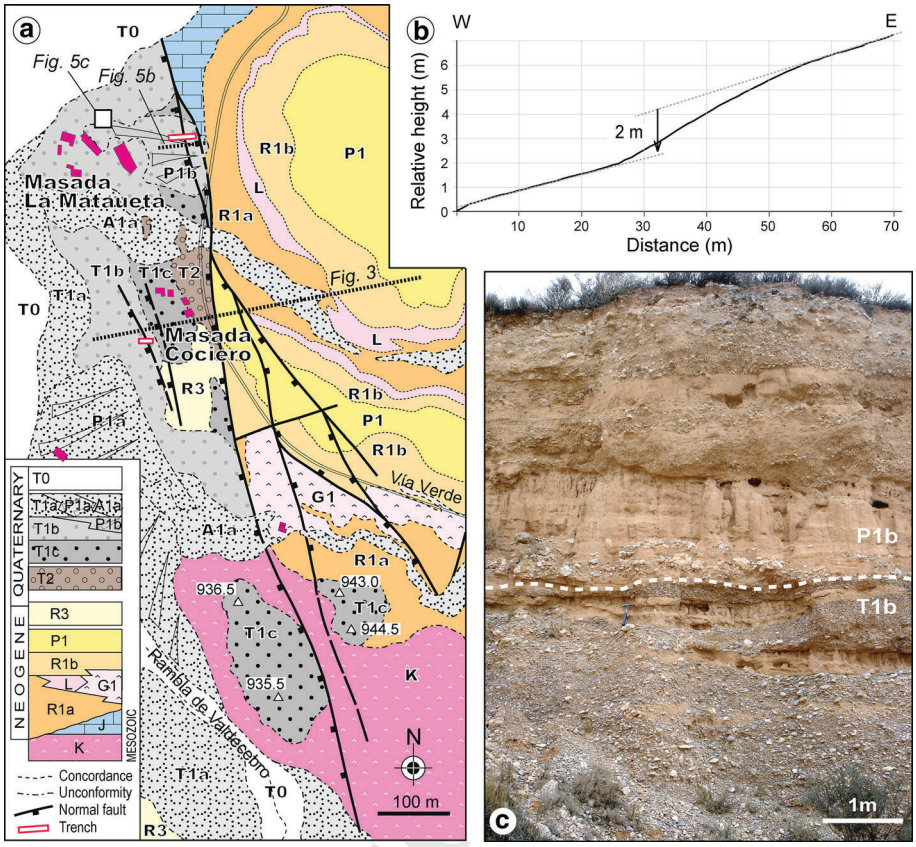

Fig. 5 **a** Detailed geological map of the southernmost sector of the Concud Fault with location of the new (Mataueta) and previous (Masada Cociero) studied trenches (see location in Fig. 2). K: Upper Triassic; J: Lower Jurassic; R1a, R1b: Vallesian clastics (Rojo 1); L: Vallesian limestone; G1: Vallesian gypsum; P1: Turolian carbonates (Páramo 1); R3: Villafranchian clastics and carbonates (Rojo 3); T2: Middle Pleistocene terrace; T1a, T1b, T1c: Late Pleistocene terraces; P1a, P1b: Late Pleistocene pediments; A1a: Late Pleistocene alluvial infill; T0: Holocene terrace/flood plain. **b** Detailed topographical profile across the surveyed fault scarp in pediment P1b. **c** Field aspect of P1b alluvial deposits overlying T1b fluvial deposits

$$P = A_{500}/A_{\text{post}P}$$

where A_{500} is the area under the probability function for the next 500 years (time between t and $t + \Delta t$ in figure 14.11 of Schwartz and Coppersmith 1986) and $A_{\text{post}P}$ is the area under the remaining part of the curve to the right of the present (t). Required input data for this procedure include the elapsed time, the average recurrence interval and its standard deviation.

4 Trenching at Mataueta site

4.1 Geological and geomorphological setting

The Mataueta trench is located 1 km from the southern tip of the Concud Fault, about 3 km north of Teruel city. It was excavated across an anomalous slope identified within a short

Journal : Small 11069 | Dispatch : 20-10-2015 | Pages : 27
Article No. : 2054 | LE | TYPESET
MS Code : NHAZ-D-14-00165 | CP | DISK

Late Pleistocene pediment on the hanging-wall block (Fig. 5a). A detailed topographical profile shows an apparent offset of the pediment surface of about 2 m (Fig. 5b). The trench followed the N 085°E direction, parallel to the maximum topographical slope and nearly orthogonal to the main fault trace.

The aforementioned pediment (P1b) links the T1c and T1b terrace sublevels, and its alluvial deposits overlie T1b fluvial deposits (Fig. 5c). Two other terrace levels are present in the hanging-wall block in the neighbouring area: T0 and T2. The latter is represented by remains of cemented gravel that crops out either at a higher topographical position close to the fault, or underlying deposits of T1c and T1b (nested terraces).

Below the aforementioned terrace and pediment deposits, two Neogene units (named Páramo 2 and Rojo 3; Late Pliocene to Early Pleistocene in age) locally crop out in the hanging-wall block. These units represent the youngest episodes of endorheic sedimentation in the Teruel Basin (Ezquerro et al. 2012). Besides, several older units (Rojo 1 and correlative units, and Páramo 1; Late Miocene) lie horizontally in the footwall of the Concud Fault. A total post-Páramo 2 unit throw of about 230 m can be calculated from the cross section in Fig. 4, which has been elaborated from map information, thickness of Neogene units in the neighbouring area and borehole data (Lafuente 2011; Lafuente et al. 2011b, 2014).

The anomalous slope detected in the P1b pediment surface does not coincide with the main trace of the Concud Fault. It runs parallel to the fault strike (NNW-SSE) some 20–25 m west of the main trace. The latter could not be trenched owing to its nearness to the *Vía Verde* touristic road. The possibility that this slope could be associated with a second rupture surface splaying from the main Concud Fault (in the same way as documented in other sectors of the structure; Lafuente 2011; Lafuente et al. 2011a, 2014) was corroborated by the geophysical results: these evidenced a linear anomaly in shallow subsoil levels that was interpreted as a steeply dipping, NNW-SSE striking fault plane cutting Late Pleistocene materials.

4.2 Materials and ages

Five sedimentary units have been distinguished (Units 1–5; Fig. 6). These units, excepting the first one, are better and more entirely represented in the hanging-wall block. After briefly describing (from bottom to top) the units, we explain how they have been correlated across the fault and we provide OSL ages.

Unit 1 Grey, grain-supported gravels with orange-greyish middle-coarse sandy matrix, laterally and vertically grading into green massive lutites. Gravels are composed by angular to subangular grey calcareous and orange siliceous pebbles with a 6 cm mean diameter, locally reaching 20 cm. There are also thin gravel levels with open framework texture. In the lower part, gravels form tabular or channelled levels, decimetric in thickness, with internal erosion surfaces and horizontal and trough cross-stratification. They are locally interbedded with fine sand beds with parallel lamination and massive lutites. The green, massive lutites form irregular levels with some interbedded dm-scale gravel bodies. Lutites include pebbles up to 13 cm in diameter (25 cm in the footwall) and are locally brown, containing white carbonate nodules that indicate pedogenesis. Rounded to subangular black limestone clasts form tabular bodies with crude horizontal stratification (gravel–fine gravel cycles) or channelled bodies with trough cross-stratification; clast diameter is lower than 2 cm (5 cm in the footwall) in the tabular bodies and up to 15 cm in the channels.

Journal : Small 11069 | Dispatch : 20-10-2015 | Pages : 27
Article No. : 2054 | ☐ LE | ☐ TYPESET
MS Code : NHAZ-D-14-00165 | ☑ CP | ☑ DISK

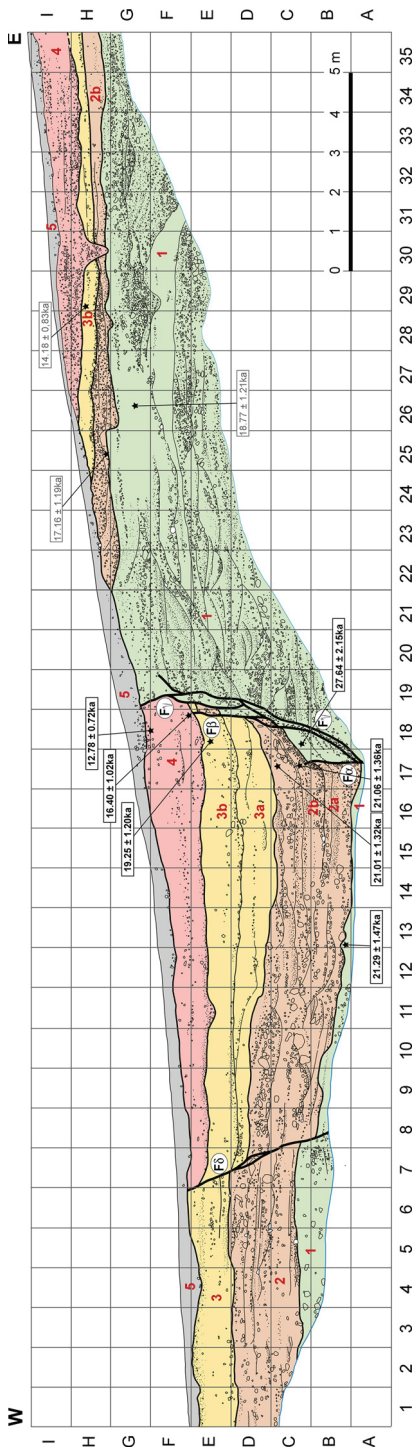

Fig. 6 Detailed log of the Matauetа trench showing location of samples for OSL dating. *Black, bold case* OSL ages considered for paleoseismic reconstruction, *grey* non-reliable, rejuvenated ages

Journal : Small 11069 | Dispatch : 20-10-2015 | Pages : 27
Article No. : 2054 | LE | TYPESET
MS Code : NHAZ-D-14-00165 | CP | DISK

Unit 2 Grey gravels in channels with internal erosion surfaces, and brown lenticular sand bodies with horizontal and planar cross-lamination. The lower part (Subunit 2a) is integrated by grey to orange grain-supported gravels with angular to subangular calcareous, and scarce siliceous clasts with diameters usually ranging from 9 to 16 cm, the biggest ones located on the base of the unit. Matrix is orange medium-size sand. Gravel forms dm-scale channelled bodies or, less commonly, lobate levels. Channels show internal erosive surfaces that separate pebble–granule–sand sequences. The upper part (Subunit 2b) is also made of gravels that, in this case, are grey to brown and intercalate levels of brown middle-coarse sands. Gravels are grain-supported, made of angular to subangular limestone pebbles up to 15 cm in diameter. Matrix is brown-orange medium-coarse sand. Similar sedimentary structures and geometry of sedimentary bodies to those in Subunit 2a are recognised. Sands form dm-scale tabular or lenticular strata, either massive or showing parallel lamination, cross-lamination and ripples.

Unit 3 Massive red silts and bad-sorted red fine sands with interbedded dm-scale, matrix-supported gravel bodies. Sands, with local calcareous pebbles, constitute cemented tabular levels up to 0.2 m thick with horizontal lamination. Gravels consist of calcareous rounded pebbles, with mean diameter of 6–8 cm, although subangular pebbles up to 15 cm are occasionally scattered through the deposit. Gravel bodies are tabular with local channelled or slightly erosive bases. One of the tabular bodies allows separating this unit into two main parts (Fig. 6): Subunit 3a, with varying thickness from 30 to 90 cm due to erosive truncation on top, and Subunit 3b, with a more homogeneous thickness, about 80–90 cm.

Unit 4 Massive red to orange silty lutites with an erosive gravel body at the bottom. The whole unit shows pedogenic evidence, displaying scattered carbonate nodules. Lutites include local angular pebbles up to 12 cm in diameter. Gravels consist of grey, matrix-supported gravels with subangular, homometric pebbles up to 15 cm in diameter, and reddish silty matrix that locally becomes greyish and microconglomeratic. They form a strongly channelled body, 0.3–0.5 m thick, which locally erodes the underlying units; moreover, it contains internal erosive surfaces and associated pebble lags.

Unit 5 Brown, poorly compacted massive lutites with scattered clasts and carbonate nodules; root bioturbation is common. It represents a very thin colluvium or regolith that has been reworked due to agricultural labours.

The described features allow interpreting these materials as deposited in a proximal alluvial system. Units 1 and 2 represented deposition in the active sector that was dominated by gravel channels and bars. Units 3 and 4 are more typical of the floodplain zone where fine terrigenous facies predominated with coarser facies only reaching this area during higher-energy flooding stages. The observed rapid lateral facies changes are typical of pediment deposits, as they are dominated by discontinuous sedimentation and shifting channels. Such facies changes and variations in thickness add some uncertainties in the correlation of Units 1–4 between both fault blocks. Aiming to support the proposed correlation (and to make optimal paleoseismological estimations), eleven samples were taken from two conspicuous lutite levels (top of Unit 1 and top of Unit 3) present at both fault blocks. Grain size and mineralogical results (Ezquerro et al. 2014) allowed confirming the initial correlation (Fig. 6). This correlation suggests that, as expected, erosive processes were dominant at the footwall block, so units were preserved only partially.

OSL dating of units has been performed from ten samples (Table 1; see location in Fig. 6). Unit 5 has not been dated because its continuous removing by farming works makes it unsuitable. OSL ages indicate that the record in the hanging-wall block of the fault has been relatively continuous and comprises from ca. 21.3 ka (top of Unit 1) to ca.

Journal : Small 11069 Dispatch : 20-10-2015 Pages : 27
Article No. : 2054 ☐ LE ☐ TYPESET
MS Code : NHAZ-D-14-00165 ☑ CP ☑ DISK

Table 1 Results of absolute OSL dating of samples collected at the Mataueta trench, as well as in a neighbouring fluvial terrace (T1c sublevel) offset by the Concud Fault

Laboratory reference	Equivalent dose (Gy)	Annual dose (mGy/year)	K factor	OSL age (years B.P.)	Sedimentary unit	Material	Location (cell in Fig. 5)
Hanging-wall block							
MAD-6164rBIN	39.18	1.84	0.12	21,293 ± 1479	Unit 1 (top)	Silt–sand	B-13
MAD-6135SDA	36.240	1.72	0.10	21,069 ± 1368	Unit 2 (middle part)	Sand	C-17I
MAD-6160SDA	43.51	2.07	0.11	21,019 ± 1329	Unit 2 (top)	Coarse sand	C-17 s
MAD-6137SDA	47.76	2.48	0.15	19,258 ± 1207	Unit 3 (top)	Silt–sand	E-18R
MAD-6133SDA	36.25	2.21	0.12	16,402 ± 1022	Unit 4 (bottom)	Silt	F-18
MAD-6134SDA	34.14	2.67	0.13	12,786 ± 723	Unit 4 (top)	Sand	G-18
Fault zone (between faults α and β)							
MAD-6136SDA	97.58	3.53	0.47	27,643 ± 2158 *	Unit 1 (top)	Lutite–silt	C-18
Footwall block							
MAD-6163rBIN	49.19	2.62	0.16	18,774 ± 1213 *	Unit 1 (top)	Silt–sand	G-26
MAD-6161rBIN	49.78	2.90	0.10	17,165 ± 1194 *	Unit 2 + 3 (bottom)	Sand with pebbles	H-25
MAD-6138SDA	40.14	2.83	0.18	14,183 ± 835 *	Unit 2 + 3 (top)	Silt–sand	H-29
T1c fluvial terrace (footwall block outside the trench)							
MAD-5778rpSDA	48.67	2.21	0.08	22,022 ± 1629	Fluvial terrace	Sand	–

The samples were analysed in Laboratorio de Datación y Radioquímica, Universidad Autónoma de Madrid, Spain. The supralinearity value in every sample is 0 Gy. Sedimentary unit, material and cell location of samples are also shown (see also Fig. 6). *Asterisks* represent ages with a likely rejuvenation process (see text for explanation)

Journal : Small 11069 | Dispatch : 20-10-2015 | Pages : 27
Article No. : 2054 | LE | TYPESET
MS Code : NHAZ-D-14-00165 | CP | DISK

12.8 ka BP (top of Unit 4). Sedimentary levels in the fault zone and in the footwall block usually provide younger OSL ages than the corresponding ones in the hanging-wall block (e.g. Units 1, 2 and 3). The position of these samples in the vicinity of erosive surfaces suggests rejuvenation processes, as discussed in detail by Ezquerro et al. (2014).

4.3 Fault geometry and kinematics

The main surveyed fault zone, with an overall trend N 165°E and dip 67°W, is made of several fault surfaces (Fig. 7). Unfortunately, no striation was observed on it, so that the precise slip vector is unknown. Nevertheless, considering the overall transport direction of the hanging wall towards N 220°E (Lafuente et al. 2011b), a virtual slip vector with a rake of 77°S could be inferred.

The hanging-wall block shows further deformation (Figs. 6, 7): (1) a single antithetic fault oriented 160/65°E and located at a distance of about 10 m from the main fault zone; (2) a gentle rollover affecting Units 1, 2 and 3a, attaining a maximum dip of 8°E.

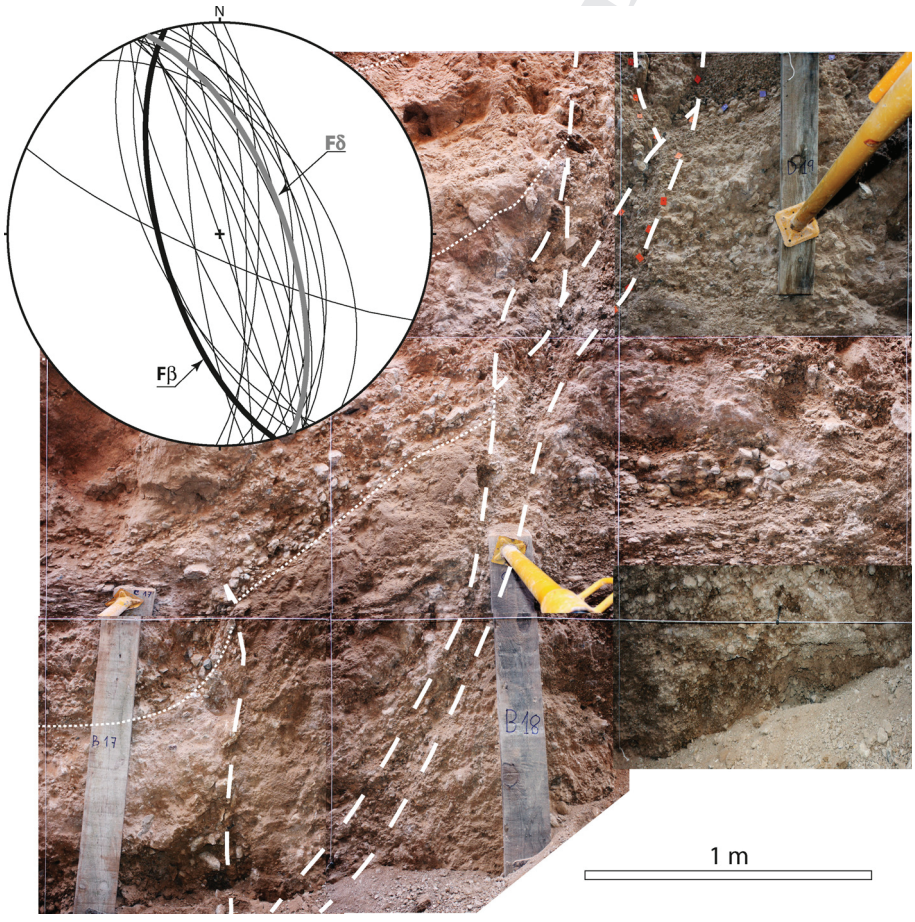

Fig. 7 Detailed trench view of the main fault zone (cell C18 and neighbouring ones, see location in Fig. 6), and stereoplot showing the orientation of measured fault planes

Journal : Small 11069 | Dispatch : 20-10-2015 | Pages : 27
Article No. : 2054 | LE | TYPESET
MS Code : NHAZ-D-14-00165 | CP | DISK

4.4 Interpretation of events

The detailed study of sedimentary units, deformation and relationship with faults allows interpreting three seismic events, with a 'creep-like' stage following the first event (Table 2). The determination of coseismic displacements is based on objective measurement of the vertical separation (throw) of discrete markers on the trench walls. The net slip values were then calculated by considering the overall dip of the fault zone (70°W) and the virtual rake of the transport direction (77°S). This resulted in a correction factor of 1.09 (net slip = throw/(sin 70° · sin 77°). As an auxiliary tool, retrodeformational analysis (Fig. 8) allowed us to construct the whole interpretation and to refine coseismic displacement values.

Event X_M Evidenced by the rupture and displacement of Subunit 2a by fault Fα, subsequently covered by Subunit 2b (Fig. 6, cells 17a,b). Subunit 2a is only present in the downthrown block, although its sedimentological features and geometrical relationship with the Fα surface suggest that it was deposited as well on the upthrown block and then completely removed due to erosion by channels at the base of Subunit 2b (Fig. 8a–c). Such hypothesised erosion would involve that the apparent measured throw $T_x = 1.2$ m (Fig. 9) is just a minimum value. The event age is bracketed between 21.3 ± 1.5 ka (Unit 1) and 21.0 ± 1.4 ka (Subunit 2b), prompting a most probable event age of 21 ka.

'Creep-like' stage The variable thickness and internal structure of Unit 3 (Fig. 6) suggests a progressive displacement along fault Fβ, mainly coeval with sedimentation of Subunit 3a. Such deformation could occur as either a creep stage or, alternatively, a succession of minor events not identifiable as characteristic earthquakes (recognising true aseismic creep in trenches is a highly complex task, submitted to great uncertainties). Probably, it also involved propagation of Fα into Subunit 2b, which would have produced the sharp (although of limited amplitude) drag fold associated with its upper, overhanging segment. Displacement along Fβ would have generated a hanging-wall rollover anticline on top of Subunit 2b, thus creating an accommodation space that was contemporary filled by Subunit 3a (Fig. 8d). Subsidence associated with this episode was comprised between 1.1 m (minimum throw on Fβ) and 1.4 m (adding the amplitude of the drag fold on Fα). Nevertheless, since it seems related to rollover accommodation, i.e. back-tilting of the downthrown block, it does not represent its true tectonic displacement (McCalpin 1996, p. 101). Subunit 3b shows more constant thickness and is locally separated from 3a by a gentle unconformity (see cell 10d in Fig. 6). Therefore, it seems to have been deposited nearly horizontal, once the rollover accommodation space had been almost completely

Table 2 Ages and throws for events distinguished in Mataueta trench

Event	Apparent throw in main fault zone (m)		Real tectonic throw (m)		Net slip (m)	Age (ka BP)		
						Predating	Postdating	Most probable
X_m	T_x	>1.2	TT_x	1.4	1.5	21.3 ± 1.5	21.0 ± 1.4	21.0
'Creep-like' stage		1.1–1.4			21.0 ± 1.3	19.2 ± 1.2	21.0 ± 19.2	
Y_m	T_y	0.7–0.9	TT_y	0.7	0.8	19.2 ± 1.2	16.4 ± 1.0	ca. 18.0
Z_m	T_z	2.6	TT_z	2.2	2.4	12.8 ± 0.7	–	post 12.8
Total		5.6–6.1		4.3	4.7			

Journal : Small 11069 | Dispatch : 20-10-2015 | Pages : 27
Article No. : 2054 | ☐ LE | ☐ TYPESET
MS Code : NHAZ-D-14-00165 | ☑ CP | ☑ DISK

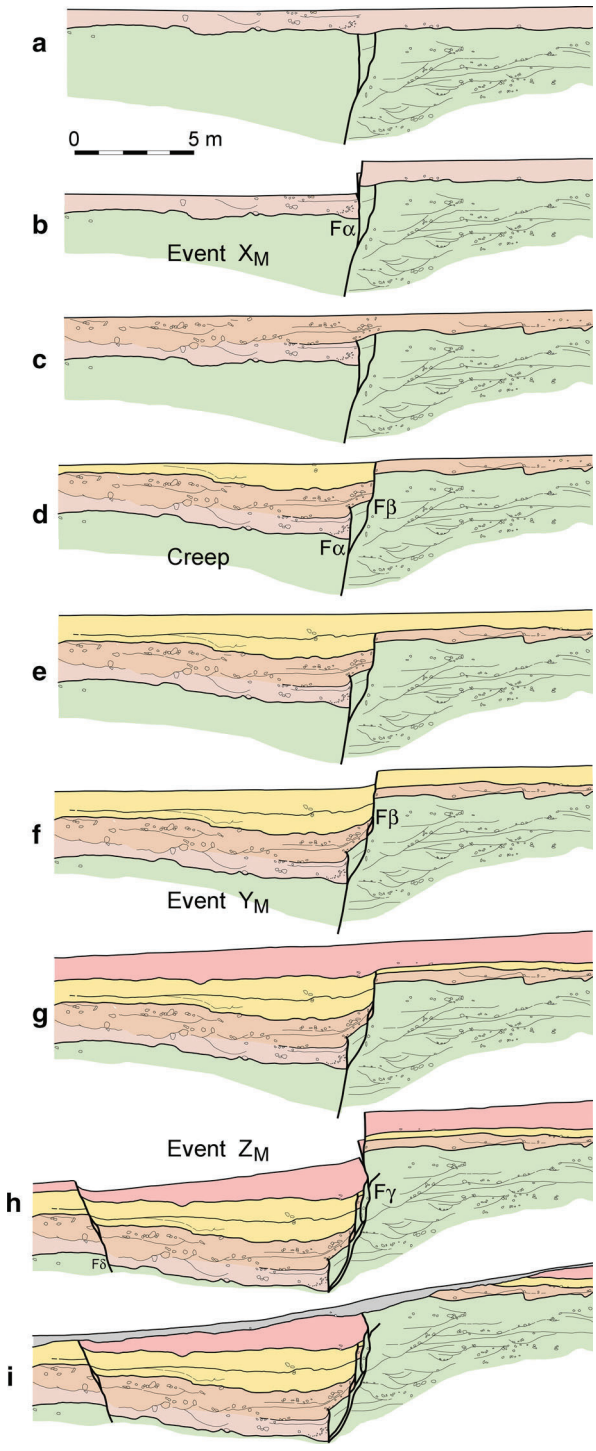

Fig. 8 Proposed evolutionary model at the Mataueta trench from retrodeformational analysis

Journal : Small 11069 | Dispatch : 20-10-2015 | Pages : 27
Article No. : 2054 | LE | TYPESET
MS Code : NHAZ-D-14-00165 | CP | DISK

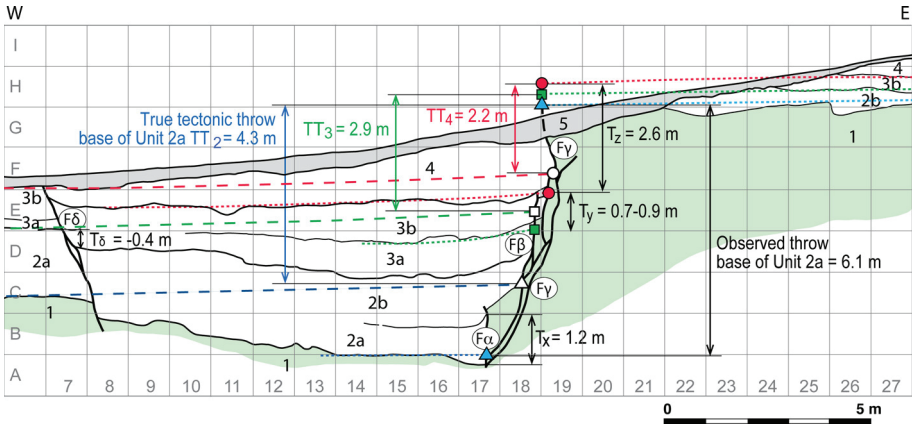

Fig. 9 Synthesis of paleoseismic interpretation at the Mataueta trench and estimation of coseismic throw values. Labels 1 to 5: sedimentary units. Fα, Fβ, Fγ, Fδ faults activated during seismic events. Solid triangle, square and circle: tip points for the base of units 2, 3 and 4, respectively (using smoothed envelopes); open triangle, square and circle: virtual tip points at the hanging block for the same markers extrapolated over the central graben. T_x, T_y, T_z: observed coseismic throws for events X_M, X_M, X_M, respectively. TT_2, TT_3, TT_4: real tectonic throws for three sedimentary markers (base of units 2, 3 and 4, respectively). Real tectonic throws for individual events (TT_x, TT_y, TT_z) are obtained as: $TT_x = TT_2 - TT_3 = 1.4$ m; $TT_y = TT_3 - TT_4 = 0.7$ m; $TT_z = TT_4 = 2.2$ m

filled (Fig. 8d, e). Thus, it can be inferred that the 'creep' stage started soon after 21.0 ± 1.3 ka (top of Subunit 2b) and finished long before 19.2 ± 1.2 ka (upper part of Subunit 3b).

Event Y_M Evidenced by displacement (with associated gentle drag folding) of Subunit 3b along fault Fβ, then buried beneath the base of Unit 4 (Figs. 6, 8f, g, cell 18b). The apparent measured throw (T_y, including drag fold) can be estimated in the range of 0.7–0.9 m (Fig. 9). Pre- and postdating ages are 19.2 ± 1.2 and 16.4 ± 1.0 ka, respectively, corresponding to samples collected at similar distances from the erosive base of Unit 4. Therefore, we consider the middle of this time range (ca. 18 ka BP) as the most probable age for this event.

Event Z_M Evidenced by displacement of Unit 4 along faults Fγ (a new rupture surface belonging to the main fault zone, cells 19f,g) and Fδ (an antithetic fault newly created during this event, cell 3e: no evidence of activity during sedimentation of previous units was found) (Figs. 6, 8h). The ensemble was then strongly eroded and covered by the subactual colluvium (Unit 5) (Fig. 8i). The throw at the base of Unit 4 has been calculated with uncertainties derived from (1) the uneven geometry of this marker, and (2) its removing in the footwall within a distance of 7 m from the main fault, which compel us to extrapolate its trace in order to measure the separation on the trench log. Using a smoothed envelope of this geologic surface in order to minimise such uncertainties, the apparent throw T_z has been measured as around 2.6 m (Fig. 9). The event age is predated by 12.8 ± 0.7 ka (upper part of Unit 4); unfortunately, no absolute postdating age is available for Unit 5.

The observed throws assigned to these three events (T_x, T_y and T_z) plus the 'creep' component broadly coeval of Subunit 3a totalise up to 6.1 m (Fig. 9), equalling the total offset exhibited by the silty level on top of Unit 1, a sedimentary marker carefully correlated between both fault blocks (Ezquerro et al. 2014). Nevertheless, they do not

Journal : Small 11069 | Dispatch : 20-10-2015 | Pages : 27
Article No. : 2054 | LE | TYPESET
MS Code : NHAZ-D-14-00165 | CP | DISK

represent their real tectonic throws. Both rollover deformation (subsidence up to 1.4 m) and slip along the antithetic fault (Tδ = 0.4 m, ascribed to event Z_M) should be interpreted as products of gravitational accommodation of the hanging-wall block. Therefore, in order to evaluate and balance the real coseismic slip values, the observed throws should be diminished by the throws associated with both structures, as stated by McCalpin (1996, p. 103) and Caputo et al. (2008). This correction can be achieved by extrapolating sedimentary markers over the graben, so defining virtual tip points at the hanging wall (open circle, square and triangle in Fig. 9). In this way, the real tectonic throw of event Z_M can be directly measured by extrapolating the base of Unit 4: $TT_Z = TT_4 = 2.2$ m (Fig. 9). This results in a net coseismic slip of $2.2 \cdot 1.09 = 2.4$ m. In the same way, real tectonic throws can be measured for the base of Unit 3 ($TT_3 = 2.9$ m) and the base of Unit 2 ($TT_2 = 4.3$ m), the last one being directly based upon the correlation of the silt level on top of Unit 1 (Ezquerro et al. 2014). Hence, we calculate the real coseismic throws associated with events Y_M and X_M: $TT_Y = TT_3–TT_4 = 0.7$ m (net coseismic slip = 0.8 m); $TT_X = TT_2–TT_3 = 1.4$ m (net coseismic slip = 1.5 m), respectively (Table 2).

5 Integrating previous and new results: paleoseismic history of the Concud Fault

So far, the paleoseismic history of the Concud Fault has been fairly known through the paleoseismological analysis of four trenches: Los Baños, Masada Cociero, El Hocino 1 and El Hocino 2 (Lafuente 2011; Lafuente et al. 2010, 2011a, 2014; Simón et al. 2012). These yielded nine events for the time lapse between ca. 74 and 15 ka BP, four of which were correlated between different trenches (events 1–8, and 10 in Fig. 10).

Based on the new information from the presented trench combined with the previous results, the paleoseismic succession was further enhanced and extended. Event X_M identified in the Mataueta trench, with the most probable age of 21 ka BP, corresponds well with event Z_{H2} of El Hocino (Lafuente et al. 2014; Fig. 10). Event Y_M, with the most probable age around 18 ka, presents some uncertainty. There are two possible interpretations in relation to the previously established paleoseismic succession. The first one is that this event corresponds to Z_{MC} at Masada Cociero trench, robustly dated to around 15 ka BP. The second one is that Y_M is distinct from Z_{MC}, so that Y_M represents an additional event between 21 and 15 ka. The second hypothesis strongly diminishes the interseismic period for the latest Pleistocene earthquakes. On the other hand, the first one requires forcing the whole error bar of the postdating age (16.4 $\pm$ 1.0 ka), involving that the age of around 15 ka for the event Y_M of Mataueta trench is more accurate than the 18 ka initially considered; furthermore, it involves that both fault branches (Mataueta and Masada Cociero) would have been activated simultaneously, so that the total net slip on the root fault would roughly equal the sum of both observed displacements (2.2 m + 0.8 m = 3.0 m). This is a value beyond both the expected and the observed ranges of coseismic slip on the Concud Fault (Lafuente et al. 2011a, 2014). Therefore, we consider the second hypothesis ($Y_M \neq Z_{MC}$) as more likely. Concerning the latest event recorded at Mataueta site (Z_M), we know that it is younger than 12.8 $\pm$ 0.7 ka, so it also represents a new, not previously defined paleoearthquake. Unfortunately, no further time constrain does exist owing to the lack of postdating age in the surveyed trench. Therefore, we can only argue that it occurred before deposition of the non-deformed Holocene terrace, with an OSL age of 3.4 $\pm$ 0.7 ka (Lafuente 2011; Lafuente et al. 2014).

Journal : Small 11069 Dispatch : 20-10-2015 Pages : 27
Article No. : 2054 LE TYPESET
MS Code : NHAZ-D-14-00165 CP DISK

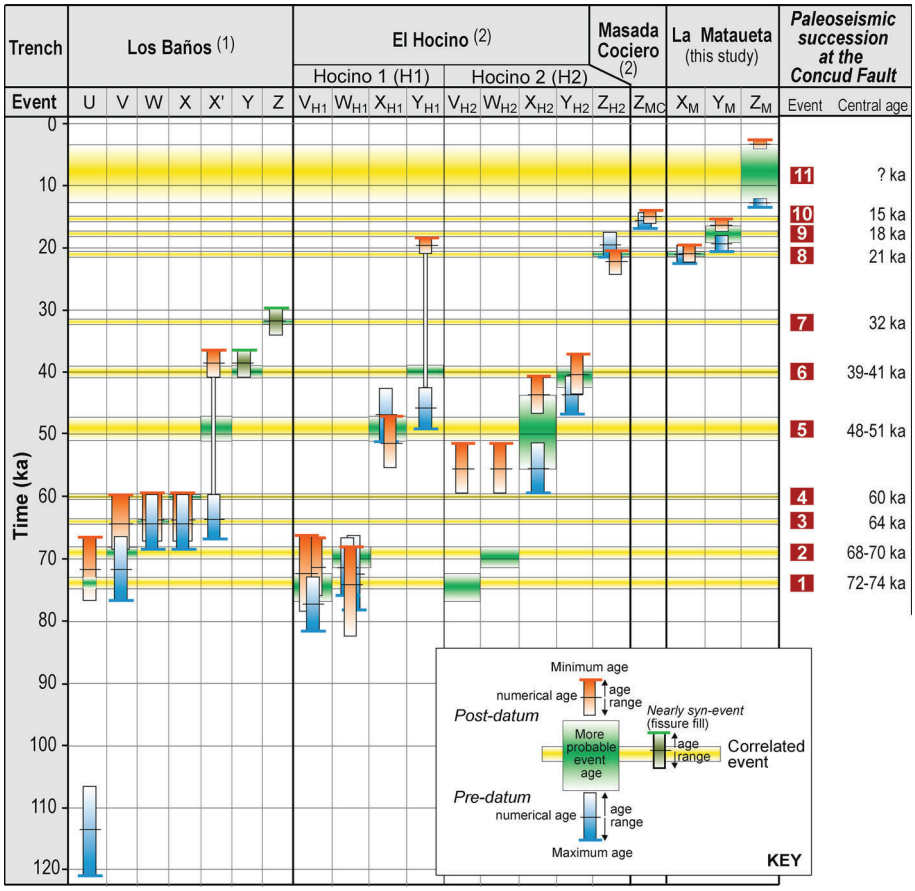

Fig. 10 Integrated paleoseismic history of the Concud Fault including events recorded at the Matagueta trench and those interpreted in the previous trenches. (1) Lafuente (2011), Lafuente et al. (2011a), (2) Lafuente (2011), Lafuente et al. (2014). Time constraints on which correlation is based are indicated in detail

In total, eleven events that have occurred since 74 ka BP were reconstructed (Figs. 10, 11). Two of them had not been detected in the previous paleoseismological studies. The total cumulative displacement is 20.5 m with an average coseismic slip of 1.9 m. Unfortunately we have not been able to establish neither the age of the last recorded event nor whether it represents the last event attributable to the Concud Fault activity. This generates some uncertainty in seismic hazard assessment, as addressed below.

The average slip rate of the fault exposed at the Matagueta trench can be obtained, as the first approach, from the net tectonic throw (4.3 m) measured from the oldest marker surveyed in the trench (base of Unit 2a, dated close to 21.3 ± 1.5 ka BP). After applying the correction factor (1.09), the resulting net tectonic slip is 4.7 m, and the net slip rate for the whole period is 0.20 ± 0.02 mm/a. If the total slip history since ca. 21 ka BP is considered for this sector of the Concud Fault, we should (1) add the coseismic slip measured at Masada Cociero (event Z_{MC}, up to 2.2 m; Lafuente et al. 2014) and (2) take into account the age range estimated for the youngest recorded event (12.8 ± 0.7 to

Journal : Small 11069 | Dispatch : 20-10-2015 | Pages : 27
Article No. : 2054 | LE | TYPESET
MS Code : NHAZ-D-14-00165 | CP | DISK

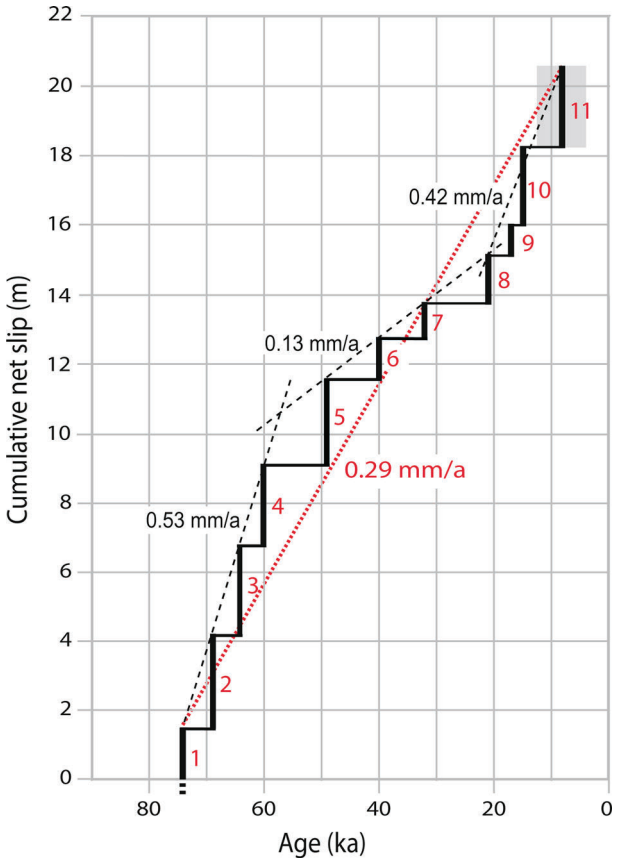

Fig. 11 Slip history of the Concud Fault, as inferred from the overall palaeoseismic results. The average slip rate for the whole recorded activity period, as well as for three successive stages, is indicated

3.4 ± 0.7 ka; absolute range 13.5–2.7 ka; mean = 8.1 ka). In this way, a slip rate ranging from 0.30 to 0.72 mm/a (mean = 0.42 mm/a) is derived for the latest recorded paleoseismic history (Fig. 11).

The slip rate during this period is higher than the average rate for the whole paleoseismic succession recorded at the Concud Fault for Late Pleistocene times (0.29 mm/a). Indeed, the overall paleoseismic pattern is characterised by alternating periods of fast slip (74.5–60 ka BP, 0.53 mm/a; 21 to ca. 8 ka BP, 0.42 mm/a) and slow slip (60–21 ka BP, 0.13 mm/a; Fig. 11).

6 Probabilistic seismic hazard analysis based on the characteristic earthquake of the Concud Fault

In seismic hazard assessment, hazard models and probability of occurrence of a given seism are obtained via the application of a recurrence model to a set of geological parameters that include slip rate, recurrence interval, displacement/event, fault geometry and elapsed time from the last paleoseismic event (McCalpin 2009).

Journal : Small 11069 | Dispatch : 20-10-2015 | Pages : 27
Article No. : 2054 | LE | TYPESET
MS Code : NHAZ-D-14-00165 | CP | DISK

Table 3 Results of probabilistic seismic hazard assessment for the characteristic earthquake of the Concud Fault

Hypothetic elapsed time (ka)	Interseismic period (average ± standard deviation, ka)	Probability of occurrence (%) of characteristic earthquake (M = 6.5–6.6) in a 500-year term
13.5	7.1 ± 3.5	26.1
8	7.3 ± 2.7	19.3
2.7	8.0 ± 3.3	2.3

Owing to the uncertainty about the age of the youngest event, three distinct hypothetic values have been considered

Previous paleoseismological studies had demonstrated that the Concud Fault has been active since the Middle Pliocene, with slip rates ranging from 0.08 to 0.33 mm/a, and potential to generate earthquakes up to $M \approx 6.8$ (Simón et al. 2005, 2012; Lafuente 2011; Lafuente et al. 2007, 2008a, b, 2010, 2011a, 2012, 2014). The total palaeoseismic succession reconstructed after those studies, and significantly expanded in the present work, includes eleven seismic events occurred since 74 ka, with a recurrence interval constrained between 7.1 ± 3.5 and 8.0 ± 3.3 ka and average coseismic displacement of 1.9 m. This succession represents a consistent activity pattern from which seismic hazard analysis based on the characteristic earthquake can be made.

The seismic potential of the Concud Fault, i.e. the moment magnitude (Mw) that can be assigned to such characteristic earthquake, is in the range of 6.4–6.8 (Lafuente 2011; Lafuente et al. 2011a). This estimation is based on its trace length (14.2 km) and its lack of segmentation and was made using empirical relations proposed by Wells and Coppersmith (1994), Stirling et al. (2002) and Pavlides and Caputo (2004). Ezquerro et al. (2015, Appendix 1) introduced the parameters of the most probable scenario for the characteristic earthquake (rupture of the total length up to a 14-km-deep detachment level, maximum coseismic slip 1.9 m) in the original equation that defines Mw (Hanks and Kanamori 1979), obtaining a range of Mw from 6.5 to 6.6.

The uncertainty about the age of the youngest event compels us to consider a number of distinct hypotheses on the *elapsed time* in order to approach the probabilistic seismic hazard: (h1) 13.5 ka, maximum value; (h2) 8 ka, arbitrary middle value; (h3) 2.7 ka, minimum value. These hypotheses give rise to three values for the average interseismic period (between 7.1 ± 3.5 and 8.0 ± 3.3 ka), as compiled in Table 3.

Assuming a probabilistic normal distribution of interseismic periods, and considering each of the three aforementioned hypotheses for the age of the youngest event, the probability of occurrence of a seism equivalent to the characteristic earthquake in a given term (500 years) has been calculated (Table 3) according to the procedure proposed by Schwartz and Coppersmith (1986). It can be seen how the elapsed time is a critical parameter, since it makes the probability to vary between 2.3 and 26.1 %.

7 Discussion

7.1 Temporal variation of slip rates

The average slip rate of the Concud Fault during Late Pliocene–Pleistocene times approaches those of other major faults in the central–eastern Iberian Chain: Sierra

Journal : Small 11069 | Dispatch : 20-10-2015 | Pages : 27
Article No. : 2054 | LE | TYPESET
MS Code : NHAZ-D-14-00165 | CP | DISK

Palomera, Calamocha, Sierra del Pobo, Teruel and Maestrat faults (all of them within the range of 0.06–0.15 mm/a; Simón et al. 2012). Nevertheless, slip rates at many of these faults tend to decay with time (particularly, at the eastern Maestrat Graben system: 0.04–0.18 mm/a for the last 3.6–5.0 Ma versus 0.02–0.05 mm/a for the last 1.9–2.6 Ma; Simón et al. 2012), while slip rate at the Concud Fault tends to increase: 0.29 mm/a in average during Late Pleistocene times (this work) versus 0.07–0.08 mm/a for the last 3.6 Ma (Lafuente 2011; Lafuente et al. 2011a). The only structure in which a comparable slip rate has been documented is the near-shore Torreblanca Fault (0.26–0.30 mm/a for the last 253.3 ± 18.0 ka; Simón et al. 2013).

Its increasing slip rate during Late Pleistocene makes the Concud Fault as active as some normal faults of the Betic Chains, e.g. Granada Fault (0.03–0.38 mm/a; Sanz de Galdeano et al. 2003) or Baza Fault (0.12–0.33 mm/a; Alfaro et al. 2008; García-Tortosa et al. 2008). This seems to be unusual if we take into account its regional setting (gentle tectonic deformation, low instrumental seismicity). Nevertheless, it could be explained if the total crustal deformation of the central–eastern Iberian Chain, formerly distributed amongst a number of large faults, was progressively concentrated into a few ones during Pleistocene times, as documented in other regions (e.g. central Apennines, Italy, since 0.9 Ma; Roberts et al. 2002). The Concud Fault could finally accommodate an important fraction of the total crustal extension at this sector of the Iberian Chain (Lafuente et al. 2014).

Such hypothesised tendency would obviously increase seismic hazard in the region surrounding the Concud Fault. The reconstructed paleoseismic succession (11 seismic events since 74 ka, with a recurrence interval constrained between 7.1 ± 3.5 and 8.0 ± 3.3 ka) represents a fairly complete record that draws a consistent activity pattern on which our hazard analysis is based. Nonetheless, we should be aware that uncertainties related to (1) temporal variation of slip rate and (2) the poorly constrained age of the last recorded event (between 13.5 and 3.4 ± 0.7 ka BP) still remain.

Temporal variation of slip rate, already pointed out in the previous studies (Lafuente et al. 2011a, 2014), is now reinforced on the basis of a more complete paleoseismic succession. The results of paleoseismological analysis of the Mataueta trench suggest the notion of a roughly cyclical activity of the fault during Late Pleistocene times. Three periods can be distinguished, two of them characterised by rapid slip (74.5–60 ka BP, 0.53 mm/a; 21 to ca. 8 ka BP, 0.42 mm/a), and separated by a period of slow slip (60–21 ka BP, 0.13 mm/a). The slip history of the Concud Fault (Fig. 11) suggests that its present-day tendency is represented by a high-activity period, with slip rate of 0.42 mm/a and average recurrence period of ca. 4.3 ka. Significantly higher seismic hazard values would be obtained by using these quantities in our probability calculations.

7.2 Characteristic earthquake model and uncertainties of seismic hazard analysis

The probabilistic hazard analysis made in the present work is based on the characteristic earthquake defined from paleoseismological study. This model assumes that (1) most strain is released in large earthquakes that fall within a narrow window of magnitude range, (2) the displacement per event at a point is nearly constant, and (3) the slip rate along strike is variable (Schwartz and Coppersmith 1984).

Other approaches, based on alternative models of fault behaviour, are possible. The perfectly periodic model (Reid 1910) postulates that earthquakes occur whenever stress builds up to a given level, and the stress drop and magnitude of each earthquake are

Journal : Small 11069 | Dispatch : 20-10-2015 | Pages : 27
Article No. : 2054 | LE | TYPESET
MS Code : NHAZ-D-14-00165 | CP | DISK

identical. If stress build-up through time is constant, the earthquakes become perfectly periodic. Shimazaki and Nakata (1980) expanded this model into the time-predictable model (quakes occur at constant critical stress level, but the stress drop and magnitude vary, the time of the next quake being predictable from the slip of the previous one) and the slip-predictable model (earthquakes fall back to a given stress level, and thus slip in the next earthquake can be predicted from the time since the previous earthquake). In order to incorporate slip variation along the fault trace, the variable and uniform slip models were proposed [see McCalpin (2009) for a review]. Variable slip models stipulate that slip rate along fault strike is constant, but that displacement per event at a point, and thus the earthquake size, is variable.

In our case, we can discard the variable slip models in benefit of the uniform slip model because the observed displacements in our paleoseismic succession are rather constant for a given site (i.e. the coefficient of variation, standard deviation/mean, at Los Baños site is 0.38 so as the mean slip is ca. 2 m, 67 % of observed slip fall between 1.2 and 2.7 m; Lafuente et al. 2011a). Amongst this family of models, most distinctions depend on the presence of persistent segments, which in the case of the Concud Fault do not exist. Thus, the characteristic earthquake model (that belongs to the uniform slip family) could be of application, as its main assumptions agree with the observed behaviour: paleoseismic observations of large displacements at trench sites, with very little evidence of smaller displacement events; near constant displacement per event in each point of the fault, but variable along its trace; and, as a result, decrease in the structural relief at the boundaries of our single-segmented fault.

Though this is probably the most favoured model amongst paleoseismologists (Liu et al. 2004), some authors have described paleoearthquake faulting chronologies that are 'non-characteristic' (Roberts 1996; Maruyama et al. 2007), which suggests that paleoseismic surveys are able to discriminate between behaviour models. Indeed, in the Teruel region, we found paleoseismic successions that include displacements significantly smaller than the mean slip at a particular site, thus deserving to be considered 'noncharacteristic' events (event of 0.1 m slip vs. mean slip of about 0.5 m at a trench in the Teruel Fault, Simon et al., in preparation). As a note of interest, such value of 0.1 m could represent very well, at least in coarse clastic sediments, a resolution threshold for event recognition under which it is not possible to identify individual events. An ensemble of discrete events whose respective displacements fall below this 'paleoseismological pixel size' could very likely be the foundation of what we have called elsewhere 'creep-like' stage.

There is not a general agreement on whether the characteristic earthquake model could successfully represent how faults in low strain regions behave. The wide gap that usually exists between the limited historical record and the long recurrence periods of such moderately active faults feeds the doubts about it. In the case of the Concud Fault, although such time gap indeed exists, a high coherency has been found between both extremes. The parameters of the characteristic earthquake of the Concud Fault (Mw $\approx$ 6.5–6.6; recurrence period $= 7.3 \pm 2.7$ ka) fit precisely the magnitude–frequency pattern obtained from the historical and instrumental seismicity of the Teruel and Jiloca grabens (Fig. 12). In our view, the whole area behaves as a homogeneous seismic zone, with a common energy dissipation pattern through seismic shakes. Part of the energy is released by multiple slip on small faults, while only scarcely the rupture of a major fault as Concud leads to the characteristic earthquake. This seismotectonic zone may be the proper domain where to interpolate between historic-instrumental and paleoseismic records. This exercise of interpolation allowed us to estimate the maximum expectable seism within a 500-year period: $M = 5.33 \pm 0.3$ (Fig. 12; Simón et al. 2014).

Journal : Small 11069 | Dispatch : 20-10-2015 | Pages : 27
Article No. : 2054 | LE | TYPESET
MS Code : NHAZ-D-14-00165 | CP | DISK

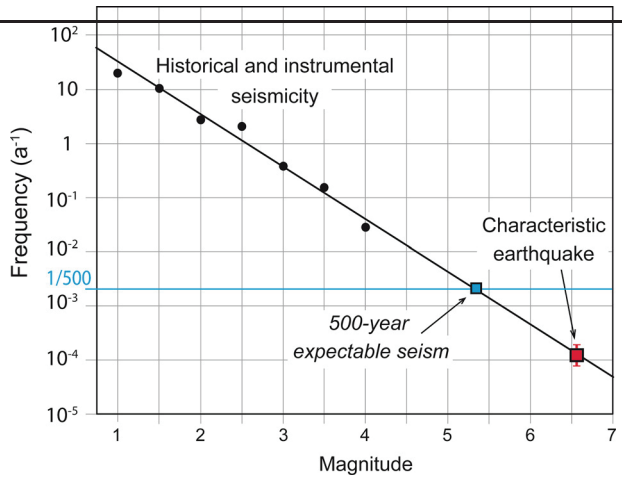

Fig. 12 Frequency–magnitude diagram for the historical and instrumental seismic activity in the Teruel area (squared in Fig. 2), showing a log-linear relationship that fits the parameters of the characteristic earthquake of the Concud Fault. Modified from Simón et al. (2014)

With respect to the elapsed time, which is of capital importance as previously shown in probabilistic modelling, it may prove to be one of the most difficult parameters to ascertain. Concerning the age of the last paleoseismic event, given that the paleoseismic history of the fault between 13.5 and 2.7 ka BP could not be reconstructed: (1) we are uncertain about the age of Z_M within this time span, and (2) we are not able to ensure that this actually represents the last one at the Concud Fault. Additional, relevant information can be obtained from the only deformed marker exposed on both fault blocks in this area. Such marker is represented by two remains of the higher sublevel of the lower terrace (T1c) present on both fault blocks, some 0.5 km SSE of Masada Cociero (Fig. 5). A post-T1c fault throw of about 8 m can be inferred from the height difference of both remains of this terrace level (943–944.5 m.a.s.l. in the footwall block; 935.5–936.5 m.a.s.l. in the hanging-wall block). The terrace remain within the hanging-wall block is now buried below the A-23 highway, but we could obtain those precise height values from the previous detailed topographical map (Ministerio de Fomento 1999, unpublished). After applying the correction factor imposed by the obliqueness of the transport direction, the estimated net tectonic slip is 8.7 m. T1c deposits within the footwall block have been dated to 22.0 ± 1.6 ka BP (Table 1) in a neighbouring outcrop some tens of metres east of the area mapped in Fig. 5. They should therefore undergo displacement due to four younger events (X_M, Y_M, Z_{MC} and Z_M), which, according to our trench studies, accumulated a total displacement of 6.9 m. The difference between both values (8.7 − 6.9 m = 1.8 m) is close to the average coseismic slip inferred from the overall paleoseismic succession (1.9 m), so it is consistent with the hypothesis of an additional, still not identified paleoseismic event. Further research is therefore required in order to refine seismic hazard assessment in the area.

7.3 Seismic hazard assessment in Teruel city

The probabilistic hazard analysis made in the present work, based on the characteristic earthquake defined from paleoseismological study of the Concud Fault, strongly differs from that one established by Spanish regulations for earthquake-resistant building up to the

Journal : Small 11069 | Dispatch : 20-10-2015 | Pages : 27
Article No. : 2054 | LE | TYPESET
MS Code : NHAZ-D-14-00165 | CP | DISK

present day (*Norma de Construcción Sismorresistente*, NCSR-02, Ministerio de Fomento 2002). Those ones only consider seismic hazard based upon historic and instrumental seismicity. The city of Teruel has been out the scope of such regulations, since the local calculated seismic acceleration for a recurrence period of 500 years was under the applicable threshold of 0.04 g.

At present, a methodological change is in progress, so that data on seismic sources (García-Mayordomo et al. 2012) are being progressively introduced into seismic hazard assessment. As a result, hazard maps published by IGN (Spanish Geographical Survey, the institution entrusted with the task of defining official seismic hazard in Spain) have been significantly modified (Solares et al. 2013), although such changes have not yet been translated into public earthquake-resistant building regulations.

A recent case pertinently illustrates how paleoseismological parameters defined here for the Concud Fault can be successfully applied to seismic hazard assessment. In 2012, the Aragón regional government presented the new project for a public hospital of Teruel, at a site 400 m far from the Concud Fault. By strict application of the current regulations, it was exempted of using the seismic-safe building practices, as stated above. Our team was tasked by the Aragón government to carry out a seismic hazard analysis based upon our knowledge of the seismic potential of the Concud Fault. In conclusions, we presented an estimate of the maximum expectable seism within a 500-year period: $M = 5.33 \pm 0.3$. Empirical correlations from this value provided a potential intensity at the hospital site of I $\geq$ VII, and a peak ground acceleration $a_p = 0.105$ g (Simón et al. 2014). In the light of our report, and because of the discrepancy with the current legal situation, the Aragón government then requested IGN and Instituto Geológico y Minero de España (IGME, the geological survey of Spain) for additional independent reports. Both institutions concluded, in a similar vein, that a seismic-safe building procedure was in order. In particular, IGN modified the seismic acceleration attributed to Teruel city and calculated a design ground acceleration (ground acceleration that derives from the basic PGA and the geotechnical conditions in site and determines appropriated building procedures in the NCSR-02 regulation) of 0.092 g (Cabañas and Solares 2013). Finally, the Aragón government decided to adapt the building project to the newly proposed seismic parameters.

8 Conclusions

Results at the presented Mataueta trench have significantly extended the paleoseismological record of the Concud Fault. Three successive events have been interpreted at minor faults splaying at a short distance from the main fault. Event X_M, with the most probable age of 21 ka BP, is correlated with event Z_{H2} previously characterised at El Hocino site (Lafuente et al. 2014). Events Y_M (ca. 18 ka) and Z_M (younger than 12.8 ± 0.7 ka, older than 3.4 ± 0.7 ka) were not identified in previous studies. Unfortunately, owing to the lack of continuous sedimentary record during Holocene times, the age of the youngest event cannot be better constrained. Neither we are confident on whether Z_M actually represents the last event in the Concud Fault; independent constraints from the offset of a neighbouring fluvial terrace support the hypothesis of an additional, still not identified paleoseismic event indeed.

After incorporating these results, the total paleoseismic succession reconstructed for the Concud Fault consists of eleven events occurred since 74.5 ka BP to the present day (Fig. 10), with an average interseismic period constrained between 7.1 ± 3.5 and

Journal : Small 11069 | Dispatch : 20-10-2015 | Pages : 27
Article No. : 2054 | LE | TYPESET
MS Code : NHAZ-D-14-00165 | CP | DISK

8.0 ± 3.3 ka. They totalise a net cumulative slip of about 20.5 m, with an average coseismic slip of 1.9 m. The average slip rate for the total recorded period is 0.29 mm/a, but the displacement pattern is characterised by alternating periods of fast slip (74.5–60 ka BP, 0.53 mm/a; 21 to ca. 8 ka BP, 0.42 mm/a) and periods of slow slip (60–21 ka BP, 0.13 mm/a).

This paleoseismic succession, together with the potential magnitude previously attributed to the characteristic earthquake at the Concud Fault ($M \approx 6.5$–6.6; Lafuente et al. 2014), has served as input for probabilistic seismic hazard analysis. Owing to the uncertainty about the age of the youngest event, three distinct hypotheses on the *elapsed time* have been considered (13.5, 8 and 2.7 ka). The estimated probability of occurrence of the characteristic earthquake in a 500-years term is 2.3, 19.3 and 26.1 %, respectively.

In spite of their uncertainties, the paleoseismological parameters defined for the Concud Fault (main potential seismic source in the area) have provided critical inputs for improving seismic hazard assessment in Teruel city.

Acknowledgments The research has been financed by project CGL2012-35662 of Spanish Ministerio de Economía y Competitividad-FEDER, as well as by the Aragón regional government (E27, Geotransfer research group). L. Ezquerro benefited from a FPI grant (BES-2010-031339) of Spanish Ministerio de Economía y Competitividad. We thank the Laboratorio de Datación y Radioquímica de la Universidad Autónoma de Madrid for OSL dating. Valuable comments by P. Stepancikova and an anonymous reviewer greatly contributed to improve the manuscript.

References

Alcalá L, Alonso-Zarza AM, Álvarez MA, Azanza B, Calvo JP, Cañaveras JC, van Dam JA, Garcés M, Krijgsman W, van der Meulen AJ, Morales J, Peláez P, Pérez-González A, Sánchez S, Sancho R, Sanz E (2000) El registro sedimentario y faunístico de las cuencas de Calatayud-Daroca y Teruel. Evolución paleoambiental y paleoclimática durante el Neógeno. Revista de la Sociedad Geológica de España 13:323–343

Alfaro P, Delgado J, Sanz de Galdeano C, Galindo-Zaldívar J, García-Tortosa FJ, López-Garrido AC, López-Casado C, Marín C, Gil A, Borque MJ (2008) The Baza Fault: a major active extensional fault in the Central Betic Cordillera (South Spain). Int J Earth Sci 97:1353–1365

Allen CR (1986) Seismological and paleoseismological techniques of research in active tectonics. In: Wallace RE (ed) Active tectonics. Studies in geophysics. National Academy Press, Washington, pp 148–154

Arlegui LE, Simón JL, Lisle RJ, Orife T (2005) Late Pliocene–Pleistocene stress field in the Teruel and Jiloca grabens (eastern Spain): contribution of a new method of stress inversion. J Struct Geol 27:693–705

Cabañas L, Solares JMM (2013) La peligrosidad sísmica en el emplazamiento del nuevo Hospital General de Teruel. Informe del IGN al Gobierno de Aragón. Unpublished

Caputo R, Pavlides S, Mucciarelli M (2008) Magnitude distribution of linear morphogenic earthquakes in the Mediterranean Region: insights from palaeoseismological and historical data. Geophys J Int 174:930–940. doi:10.1111/j.1365-246X.2008.03834.x

Ezquerro L, Lafuente P, Pesquero MD, Alcalá L, Arlegui LE, Liesa CL, Luque L, Rodríguez-Pascua MA, Simón JL (2012) Una cubeta endorreica residual del Pleistoceno inferior en la zona de relevo entre las fallas neógenas de Concud y Teruel, Cordillera Ibérica: implicaciones paleogeográficas. Revista de la Sociedad Geológica de España 25:157–175

Ezquerro L, Liesa CL, Simón JL, Arlegui L, Luzón A, Lafuente P (2014) Correlation of sedimentary units from grain-size and mineralogic analyses as a tool for constraining trench interpretation in paleoseismology. Int J Earth Sci 103:2327–2333

AQ4 Ezquerro L, Moretti M, Liesa CL, Luzón A, Simón JL (2015) Seismites from a well core of palustrine deposits as a tool for reconstructing the palaeoseismic history of a fault. Tectonophysics (in press)

García-Mayordomo J, Insua-Arévalo JM, Martínez-Díaz JJ, Jiménez-Díaz A, Martín-Banda R, Martín-Alfageme S, Álvarez-Gómez JA, Rodríguez-Peces M, Pérez-López R, Rodríguez-Pascua MA, Masana

Journal : Small 11069 | Dispatch : 20-10-2015 | Pages : 27
Article No. : 2054 | LE | TYPESET
MS Code : NHAZ-D-14-00165 | CP | DISK

E, Perea H, Martín-González F, Giner-Robles J, Nemser ES, Cabral J, QAFI compilers (2012) The quaternary active faults database of Iberia (QAFI v.2.0). J Iberian Geol 38(1):285–302

García-Tortosa FJ, Sanz de Galdeano C, Sánchez-Gómez M, Alfaro P (2008) Geomorphologic evidence of the active Baza Fault (Betic Cordillera, South Spain). Geomorphology 97:374–391

Godoy A, Ramírez JI, Olivé A, Moissenet E, Aznar JM, Aragonés E, Aguilar MJ, Ramírez del Pozo J, Leal MC, Jerez-Mir L, Adrover R, Goy A, Comas MJ, Alberdi MT, Giner J, Gutiérrez-Elorza M, Portero JM, Gabaldón V (1983a) Mapa Geológico de España 1:50.000, hoja no 567 (Teruel) y memoria. IGME, Madrid

Godoy A, Olivé A, Moissenet E (1983b) Mapa Geológico de España 1:50.000, hoja no 542 (Alfambra) y memoria. IGME, Madrid

Gutiérrez M, Peña JL (1976) Glacis y terrazas en el curso medio del río Alfambra (provincia de Teruel). Boletín Geológico y Minero 87:561–570

Gutiérrez F, Gutiérrez M, Gracia FJ, McCalpin JP, Lucha P, Guerrero J (2008) Plio-quaternary extensional seismotectonics and drainage network development in the central sector of the Iberian Range (NE Spain). Geomorphology 102:21–42

Hanks TC, Kanamori H (1979) A moment magnitude scale. J Geophys Res 84:2348–2350

Herraiz M, De Vicente G, Lindo-Ñaupari R, Giner J, Simón JL, González-Casado JM, Vadillo O, Rodríguez-Pascua MA, Cicuéndez JI, Casas A, Cabañas L, Rincón P, Cortés AL, Ramírez M, Lucini M (2000) The recent (upper Miocene to Quaternary) and present tectonic stress distributions in the Iberian Peninsula. Tectonics 19:762–786

IGN (2010) Servicio de Información Sísmica del Instituto Geográfico Nacional. http://www.ign.es/ign/es/IGN/SisCatalogo.jsp. Accessed December 2010

Lafuente P (2011) Tectónica activa y paleosismicidad de la falla de Concud (Cordillera Ibérica central). Ph.D. Thesis, Universidad de Zaragoza

Lafuente P, Simón JL, Rodríguez-Pascua MA, Arlegui LE, Liesa CL (2007) Aproximación al comportamiento paleosísmico de la falla de Concud (Teruel, Cordillera Ibérica). Actas III Congreso Nacional de Ingeniería Sísmica, Girona, Asociación Española de Ingeniería Sísmica, pp 211–223

Lafuente P, Lamelas T, Soriano MA (2008a) Caracterización morfotectónica de la actividad de la falla de Concud (Cordillera Ibérica, Teruel). Geo-Temas 10:1027–1030

Lafuente P, Rodríguez-Pascua MA, Simón JL, Arlegui LE, Liesa CL (2008b) Sismitas en depósitos pliocenos y pleistocenos de la fosa de Teruel. Revista de la Sociedad Geológica de España 21:133–149

Lafuente P, Arlegui LE, Liesa CL, Simón JL (2010) Nuevo estudio paleosismológico en el sector central de la falla de Concud (fosa del Jiloca, Teruel): resultados preliminares. In: Insua JM, Martín-González F (eds) Contribución de la Geología al Análisis de la Peligrosidad Sísmica, Sigüenza (Guadalajara, España), pp 67–70

Lafuente P, Arlegui LE, Liesa CL, Simón JL (2011a) Paleoseismological analysis of an intraplate extensional structure: the Concud fault (Iberian Chain, Spain). Int J Earth Sci 100:1713–1732. doi:10.1007/s00531-010-0542-1

Lafuente P, Arlegui LE, Casado I, Ezquerro L, Liesa CL, Pueyo Ó, Simón JL (2011b) Geometría y cinemática de la zona de relevo entre las fallas neógeno-cuaternarias de Concud y Teruel (Cordillera Ibérica). Revista de la Sociedad Geológica de España 24:117–132

Lafuente P, Arlegui LE, Liesa CL, Simón JL (2012) Reply to the discussion by F Gutiérrez, P Lucha, J Guerrero, M Gutiérrez and D Carbonel on the article "Paleoseismological analysis of an intraplate extensional structure: the Concud fault (Iberian Chain, Spain)". Int J Earth Sci 101:587–594. doi:10.1007/s00531-011-0661-3

Lafuente P, Arlegui LE, Liesa CL, Pueyo Ó, Simón JL (2014) Spatial and temporal variation of palaeoseismic activity at an intraplate, historically quiescent structure: the Concud fault (Iberian Chain, Spain). Tectonophysics 632:167–187

Liu L, Zoback MD (1997) Lithospheric strength and intraplate seismicity in the New Madrid seismic zone. Tectonics 16:585–595

Liu J, Klinger Y, Sieh K, Rubin C (2004) Six similar sequential ruptures of the San Andreas fault, Carrizo Plain, California. Geology 32:649–652

Maruyama T, Iemura K, Azuma T, Yoshioka T, Sato M, Miyawaki R (2007) Paleoseismological evidence for non-characteristic behavior of surface rupture associated with the 2004 Mid-Niigata Prefecture earthquake, central Japan. Tectonophysics 429:45–60

McCalpin JP (1996) Paleoseismology. Academic Press, New York

AQ5 McCalpin JP (2009) Paleoseismology, 2nd edn. International Geophysics Series, vol 95. Elsevier

Mezcua J, Martínez-Solares JM (1983) Sismicidad del Área Ibero-Mogrebí. IGN, Madrid

Ministerio de Fomento (2002) Real Decreto 997/2002, de 27 de septiembre, por el que se aprueba la norma de construcción sismorresistente: parte general y edificación (NCSR-02). BOE 244:35898–35967

Journal : Small 11069 | Dispatch : 20-10-2015 | Pages : 27
Article No. : 2054 | LE | TYPESET
MS Code : NHAZ-D-14-00165 | CP | DISK

Moissenet E (1982) Le Villafranchien de la région de Teruel (Espagne). Stratigraphie-deformations-milieux. Colloque "Le Villafranchien méditerranéen", Lille, pp 229–253

Opdyke N, Mein P, Lindsay E, Pérez-González A, Moissenet E, Norton VL (1997) Continental deposits, magnetostratigraphy and vertebrate paleontology, late Neogene of Eastern Spain. Palaeogeogr Palaeoclimatol Palaeoecol 133:129–148

Pavlides S, Caputo R (2004) Magnitude versus faults' surface parameters: quantitative relationships from the Aegean Region. Tectonophysics 380:159–188

Peña JL (1981) Las acumulaciones cuaternarias de la confluencia de los ríos Alfambra y Guadalaviar, en las cercanías de Teruel. Actas VII Coloquio de Geografía, Pamplona, pp 255–259

Peña JL, Gutiérrez M, Ibáñez MJ, Lozano MV, Rodríguez J, Sánchez M, Simón JL, Soriano MA, Yetano LM (1984) Geomorfología de la provincia de Teruel. Instituto de Estudios Turolenses, Teruel

Reid HF (1910) The Mechanics of the Earthquake, The California Earthquake of April 18, 1906, Report of the State Investigation Commission, vol 2. Carnegie Institution of Washington, Washington, DC

Rhoades DA, van Dissen RJ (2003) Estimates of the time-varying hazard of rupture of the Alpine Fault, New Zealand, allowing for uncertainties. NZ J Geol Geophys 46:479–488

Roberts GP (1996) Noncharacteristic normal faulting surface ruptures from the Gulf of Corinth, Greece. J Geophys Res 101:25255–25267

Roberts GP, Michetti AM, Cowie P, Nigel C, Morewood NC, Papanikolaou I (2002) Fault slip-rate variations during crustal-scale strain localisation, central Italy. Geophys Res Lett. doi:10.1029/2001GL013529

Roca E, Guimerà J (1992) The Neogene structure of the eastern Iberian margin: structural constraints on the crustal evolution of the Valencia trough (western Mediterranean). Tectonophysics 203:203–218

Rubio JC, Simón JL (2007) Tectonic subsidence v. erosional lowering in a controversial intramontane depression: the Jiloca basin (Iberian Chain, Spain). Geol Mag 144:1–15

Sanz de Galdeano C, Peláez JA, López-Casado C (2003) Seismic potential of the main active faults in the Granada Basin (Southern Spain). Pure appl Geophys 160:1537–1556

Schwartz DP, Coppersmith KJ (1984) Fault behaviour and characteristic earthquakes: examples form the Wasatch and San Andreas Faults. J Geophys Res 89:5681–5698

Schwartz DP, Coppersmith KJ (1986) Seismic hazards: new trends in analysis using geologic data. In: Active tectonics: studies in geophysics (RE Wallace, Chairperson). National Academic Press, Washington DC, pp 215–230

Shimazaki K, Nakata T (1980) Time-predictable recurrence model for large earthquakes. Geophys Res Lett. doi:10.1029/GL007i004p00279

Simón JL (1983) Tectónica y neotectónica del sistema de fosas de Teruel. Teruel 69:21–97

Simón JL (1989) Late Cenozoic stress field and fracturing in the Iberian Chain and Ebro Basin (Spain). J Struct Geol 11:285–294

Simón JL, Lafuente P, Arlegui LE, Liesa CL, Soriano MA (2005) Caracterización paleosísmica preliminar de la falla de Concud (fosa del Jiloca, Teruel). Geogaceta 38:63–66

Simón JL, Arlegui LE, Lafuente P, Liesa CL (2012) Active extensional faults in the central-eastern Iberian Chain, Spain. J Iber Geol 38:127–144

Simón JL, Pérez-Cueva AJ, Calvo-Cases A (2013) Tectonic beheading of fluvial valleys in the Maestrat grabens (eastern Spain): insights into slip rates of Pleistocene extensional faults. Tectonophysics 593:73–84

Simón JL, Arlegui LE, Ezquerro L, Lafuente P, Liesa CL (2014) Aproximación a la peligrosidad sísmica en la ciudad de Teruel asociada a la falla de Concud (NE España). Geogaceta 56:7–10

Solares JMM, Cabañas L, Benito MB, Ribas A, Gaspar JM, Ruiz S, Rodríguez O (2013) Actualización de mapas de peligrosidad sísmica de España 2012. Centro Nacional de Información Geográfica (CNIG), Madrid

Stirling M, Rhoades D, Berryman K (2002) Comparison earthquake scaling relations derived from data of the instrumental and preinstrumental era. Bull Seismol Soc Am 92(2):820–830

Wells DL, Coppersmith KJ (1994) New empirical relationships among magnitude, rupture length, rupture width, rupture area, and surface displacement. Bull Seismol Soc Am 84(4):974–1002

Yeats RS, Sieh K, Allen CR (1997) The geology of earthquakes. Oxford University Press, New York

Journal : **11069**
Article : **2054**

Springer
the language of science

Author Proof

Author Query Form

Please ensure you fill out your response to the queries raised below and return this form along with your corrections

Dear Author

During the process of typesetting your article, the following queries have arisen. Please check your typeset proof carefully against the queries listed below and mark the necessary changes either directly on the proof/online grid or in the 'Author's response' area provided below

Query	Details Required	Author's Response
AQ1	Kindly check and confirm the corresponding author is correctly identified and amend if necessary.	
AQ2	Please check whether the mail ID 'palomalt@unizar.es' should appear in the publication.	
AQ3	Please suggest whether the terms such as 'paleoseismic' and 'paleoseismology' can be changed to 'palaeoseismic' and 'palaeoseismology', respectively, throughout the article.	
AQ4	Kindly provide volume number and page range for reference Ezquerro et al. (2015).	
AQ5	Kindly provide publisher location for reference McCalpin (2009).	